

## DENT-TO-STIFFENER EVALUATION CONCEPT FOR THIN-WALLED STEEL CYLINDERS

Oğuzhan AKARSU <sup>a</sup>, Barış BAYRAK <sup>b</sup>, Mahmut KILIÇ <sup>c</sup>, Mahyar MAALI <sup>d</sup>, Abdulkadir Cüneyt AYDIN <sup>e\*</sup>

<sup>a</sup> PhD Student; Ataturk University, Engineering Faculty, Department of Civil Engineering, 25030, Erzurum, Turkey

<sup>b</sup> Dr; Kafkas University, Engineering & Architecture Faculty, Department of Civil Engineering, Kars, Turkey

<sup>c</sup> Assoc. Prof.; Ataturk University, Engineering Faculty, Department of Civil Engineering, 25030, Erzurum, Turkey

<sup>d</sup> Assoc. Prof.; Erzurum Technical University, Engineering & Architecture Faculty, Department of Civil Engineering, 25050, Erzurum, Turkey

<sup>e</sup> Prof.; Ataturk University, Engineering Faculty, Department of Civil Engineering, 25030, Erzurum, Turkey

\*E-mail address: [acaydin@atauni.edu.tr](mailto:acaydin@atauni.edu.tr)

Received: 20.09.2022; Revised: 26.05.2023; Accepted: 16.06.2023

### Abstract

Defects/imperfections can occur during manufacturing, assembly, welding, and other processes, which can reduce the critical buckling load. However, the axial buckling load is beyond the scope of this work, and there are many studies on the stiffening effect of longitudinal dents. This concept combined the idea of the dent-to-stiffener evaluation concept for thin-walled steel cylinders. This study aims to transform the dents into artificial dents for a stiffening effect on the buckling phenomena. For this purpose, 37 thin-walled steel cylinder models, including the perfect model, were designed for varying dent shapes, dent widths, dent depths, dent lengths, and dent angles. The study also contributed to the effect of dent parameters on the critical buckling load of thin-walled steel cylinders. In particular, increasing the initial buckling will motivate the industry to convert dents into stiffeners with small artificial touches to enhance the longevity of the structure. The results showed that the introduction of certain artificial dents can significantly increase the critical buckling load of cylinders, thus improving their resistance against buckling, which has significant implications for various industries that use thin-walled steel cylinders in their structures. The proposed simulations for transforming dents into artificial stiffeners can be a valuable tool for enhancing the longevity and safety of thin-walled steel cylinders and other structures.

**Keywords:** Dent shape; External pressure; Imperfection effect; Stiffener; Thin-walled.

## 1. INTRODUCTION

Buckling is one of the worst failure modes of unstiffened cylindrical shells under external pressure. Thus, it is crucial to design such cylinders according to the buckling conditions. Defects/imperfections can occur during manufacturing, assembly, welding, and other processes, which can reduce the critical buckling load. Dented cylinders can no longer support the load acting on the structure before buckling. Theoretical and experimental studies on shell structures have been conducted since the 18<sup>th</sup> century [1–3]. Koiter pioneered the investigation of the stability of cylindrical shells and the effect of imperfections on buckling [4].

During this period, different codes and standards were developed. Different codes and standards regarding critical buckling pressures are included in Jawad, Ross, Ventsel and Krauthaer's theory, the British Standards Institution Code, the European Recommendations Code, and NASA SP-8007. Several studies have been conducted on the buckling reaction of cylindrical shell structures with dent-related imperfections under external pressure [5–12]. Ghazijahani et al. and Rathinam and Prabu that certain imperfections increase the critical buckling pressure of the cylindrical shell slightly more than that of a perfect cylindrical shell [13, 14]. The main factors

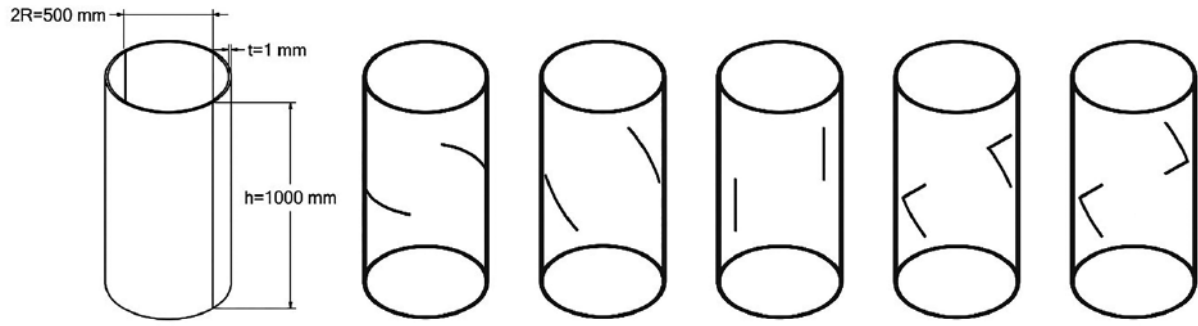


Figure 1.  
Cylinder geometry properties and dent shape

Table 1.  
Material Properties [12]

Material	Yield stresses (MPa)	Tangent Modulus (MPa)	Young's modulus (MPa)	Poisson's ratio
Cylinder sheet	198.8	1450	210 000	0.29

affecting the collapse pressure of circular cylindrical shells are the H/R aspect ratio (height of the shell to the radius) and slenderness ratio (the ratio of the radius to the thickness of the shell) [8, 15].

In this paper, a parametric study based on the dent shape (dent angle, dent length, dent depth, and dent width) is carried out to determine which type of dents can be artificially improved to increase the critical buckling load of the thin-walled steel cylindric shell. Numerical models are generated with centrally located double dents for the symmetry concept. The models are grouped as “0, 45, 90, <-< and <->” according to their dent shapes. The models were designed according to four different dents heights, two different dents widths, and four different dents depths. All the models had an H/R value of 2 and an R/t value of 250. FE results were compared with Jawad, Ross, Ventsel and Krauthaer's theory and NASA SP-8007. The equations used in the calculations are as follows:

$$\text{Jawad Theory [16]: } P_j = \frac{0.92E \left(\frac{t}{R}\right)^{2.5}}{h_c / R} \quad (1)$$

$$\text{Ross Theory [17]: } P_r = \frac{2.6E \left(\frac{t}{2R}\right)^{2.5}}{\frac{h_c}{2R} - 0.45 \left(\frac{t}{2R}\right)^{0.5}} \quad (2)$$

$$\text{Ventsel and Krauthaer [18]: } P_r = \frac{2.6E \left(\frac{t}{2R}\right)^{2.5}}{\frac{h_c}{2R} - 0.45 \left(\frac{t}{2R}\right)^{0.5}} \quad (3)$$

$$\text{NASA SP-8007 [19]: } P_{SP-8007} = 0.9P_{LBA} \quad (4)$$

The circumferential buckling wave number is calculated through approximations by Teng et al. [20].

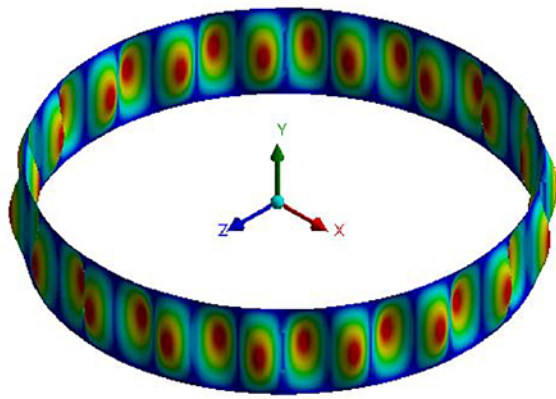
$$n = 2.74 \sqrt{\frac{R}{h_c} \sqrt{\frac{R}{t}}} \quad (5)$$

## 2. NUMERICAL MODELING

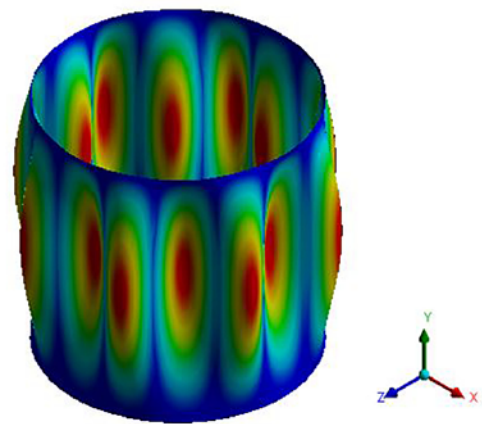
This study is a continuation of a previous study that investigated both the experimental and numerical defects [21]. The cylindrical shells are modelled using shell elements (with an element size of 7.5 mm and a structured quadrilateral mesh), along with triangular elements, in ANSYS [22]. Also, more precise mesh sizes were used for dents. By utilizing this element, it is possible to handle the membrane, bending, and transverse shear effects, as well as satisfactorily form curvilinear surfaces. Furthermore, this element exhibited plasticity, stress stiffening, and large deflection and strain capabilities. The analytical figures for the models are 10 times greater.

### 2.1. Geometry and Material

In this section, a series of dented shells are introduced which represent cylindrical shells. The cylindrical shells are burdened by external pressure. The height and diameter of the cylindrical models are fixed in all models, the height is determined as 1000 mm and the radius is 250 mm. In the models, 5 different types of dents were examined. Different parameters such as dent depth, width, height, angle, and shape were selected as dent types. The dent shapes are shown in Fig. 1. In all models, two dents are cen-



a Combescure and Gusic



b Windernburg and Trilling

Figure 2.

(a) First eigen buckling mode shape in the isometric view of the model A given in Combescure and Gusic [27]. (b) First eigen buckling mode shape in the isometric view of model 53 given in Windernburg and Trilling [28]

trally and symmetrically placed. The dent depth in models in all groups was taken as  $t$  (shell thickness) and  $2t$ . The dent lengths in the models were determined as  $h/4$ ,  $h/3$ ,  $h/2$ ,  $3h/4$ . The first group has dents at 0 degrees and includes models M1 to M6. Dents are intertwined in models with 0 degree and  $3h/4$  length. Therefore, it is not included in the results. The second group has dents at a 45-degree angle and includes models M7 to M12. In models with 45 degrees group, V, and inverted V dents, the dent lengths are considered for the vertical distance. The third group has 90-degree dents and includes models M13 to M20. V-shaped dents were examined in the fourth and fifth groups. While the V shape is in the same direction in the fourth group, they are in the opposite direction in the fifth group. Information regarding the geometries of the models is given in Table 4, Table 5, Table 6, Table 7, and Table 8. Two factors were carefully considered when modelling localized geometric imperfections, such as dents. The first is the accurate modelling of the dent shape, and the second is the need for careful modelling of the surrounding region in shell structures, where there is a change in curvature, as this can cause local bending stresses [23–25]. The core concepts that underlie contemporary design codes for metallic structures were

primarily established through the examination of bilinear material behaviour, which entails an elastic response followed by a perfectly plastic one [26]. The properties of AISI 316 stainless steel, characterized as a bilinear isotropic material with a tangent modulus (ET), are provided in Table 1. The values presented in the table were derived from the investigation conducted by Korucuk (2019).

## 2.2. Model Validation

The critical buckling pressures were compared with the Combescure and Gusic [27] and Windernburg and Trilling [28] studies given in the Rathinam and Prabu [13] study to validate the FE model with the current study results. The model geometries, material properties and Critical buckling pressure are listed in Table 2 and Table 3. Fig. 2 shows the results of the analysis.

### 2.2.1. Boundary condition

All the nodes in the bottom edge (i.e., at  $y=0$ , with reference to the coordinate system shown in Fig. 2(a)) were restrained from moving in the  $x$ ,  $y$ , and  $z$ -directions, and all the nodes in the top support edges were restrained from moving in the  $x$  and  $z$ -directions only.

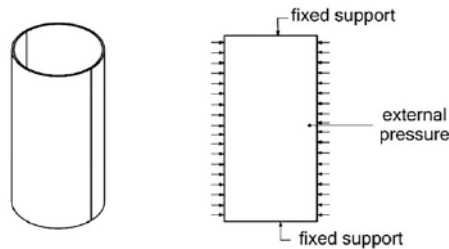
Table 2.

Comparison with buckling pressure of the cylindrical shell given in Combescure and Gusic [27] and Rathinam and Prabu [13]

Cylindrical shell	R (mm)	L (mm)	t (mm)	Young's modulus (GPa)	Poisson's ratio ( $\nu$ )	FE eigen buckling pressure (MPa)		
						Combescure and Gusic	Rathinam and Prabu	From present analysis
A	50	20	0.15	200	0.3	0.2936	0.2927	0.2985

**Table 3.**  
Comparison with buckling pressure of the cylindrical shell given in Windernburg and Trilling [28] and Rathinam and Prabu [13]

Cylindrical shell	R (mm)	L (mm)	t (mm)	Young's modulus (GPa)	Poisson's ratio ( $\nu$ )	FE eigen buckling pressure (MPa)		
						Windernburg and Trilling	Rathinam and Prabu	From present analysis
53	203.2	406.4	0.8	193	0.3	0.096 (8)	0.108 (8)	0.111 (8)



**Figure 3.**  
Boundary condition

### 2.3. Boundary Conditions and Solution Algorithm

Radial restraint is known as the main effective edge restraint in thin-walled cylindrical shells. The top and bottom edges in all models were fixed supported with only radial restraint. Clamped boundary conditions (see Fig. 3) are applied. The bottom and top edges of the cylindrical models were restrained against radial displacements. Uniform external pressure was applied to the entire surface of the cylindrical shells. Mesh and convergence correction studies were performed to ensure the high accuracy of the analysis.

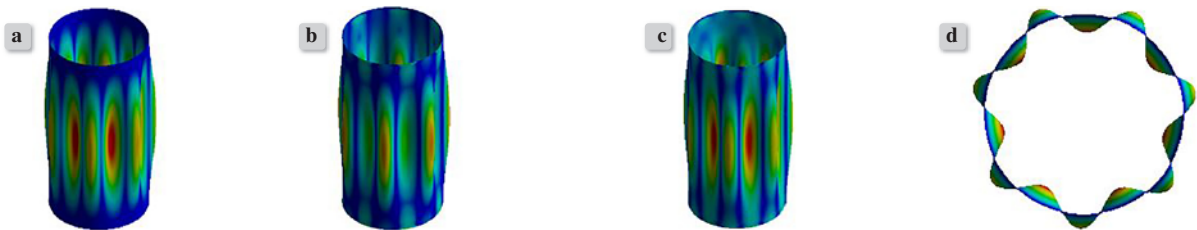
Geometric and material nonlinear analysis with imperfections (GMNIA) was utilized to determine the buckling resistance of the cylindrical shells under investigation. Nonlinear analysis was carried out using the full Newton-Raphson approach. Energy-based stabilization techniques available in ANSYS were used to ensure convergence. The energy dissipation ratio was assumed to be in the stabilization range, with the stabilization energy never exceeding 1% of the total potential energy. Within nonlinear numerical computations, geometric imperfections and nonlinear material models were employed. The outcome of the nonlinear analysis represents the behaviour of the structure by means of a load-dis-

placement path related to the selected boundary conditions and the analyzed load while considering the effect of elastoplastic instability. Nonlinear materials were used in all the models. Except for the M37 model, all models were geometrically imperfect, and the M37 model was designed perfectly.

### 3. RESULTS

First, the critical buckling results of the perfect model were obtained. The results of the perfect model (M37) are given in Fig. 4 and Fig. 5. Theoretical formulas are evaluated for perfect shells. The critical buckling pressures calculated according to the theoretical formulations were between 48.9–65.2. The critical buckling pressure of the perfect model was approximately 60.1 kPa. The wave number was obtained from Teng's formula as approximately 6. The wave number of the perfect model (M37) was 7. Fig. 4 demonstrates the FE results of the perfect model. In Fig. 5, the results of the perfect model before-initial-post buckling are shown.

Consequently, three dent forms that enhance the critical buckling pressure were determined according to the perfect model. These were the M3 and M6 models with a dent along the entire circumference and the M8 model with a 45-degree angle. The FE results showed that the dent shapes with the highest critical buckling pressures were the 0°-angle dent shapes. If we evaluate the dent widths, in the first group (0°-angle dent), the critical buckling pressure value decreased as the dent width increased between M1 and M4, M2 and M5. From M3 to M6, the increase in the dent width increased the critical buckling pressure by 6%. In this group, the increase in dent length from  $h/4$  to  $h/3$  (from M1 to M2 and M4 to M5) caused a decrease in



**Figure 4.**  
Perfect Model (M37), a) Total deformation b) Maximum principal strains c) Von Mises stress d) Waveform



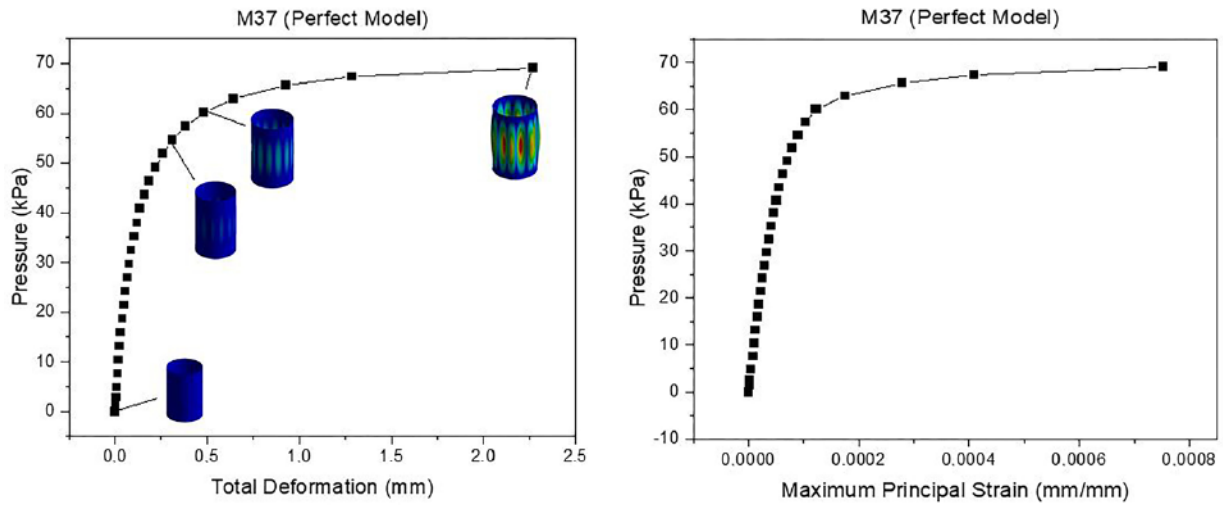


Figure 5.  
Perfect model (M37) results

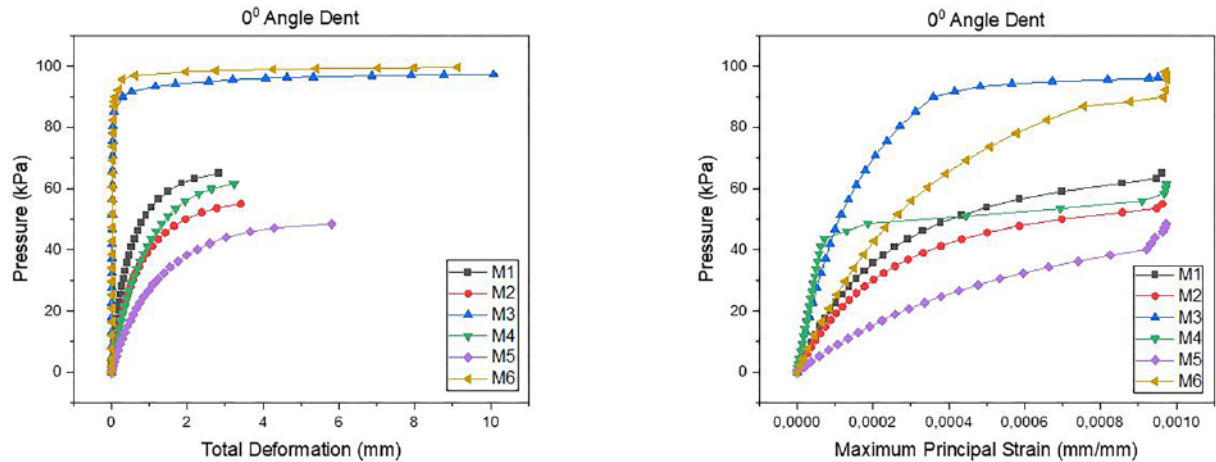


Figure 6.  
0°-angle dent group results

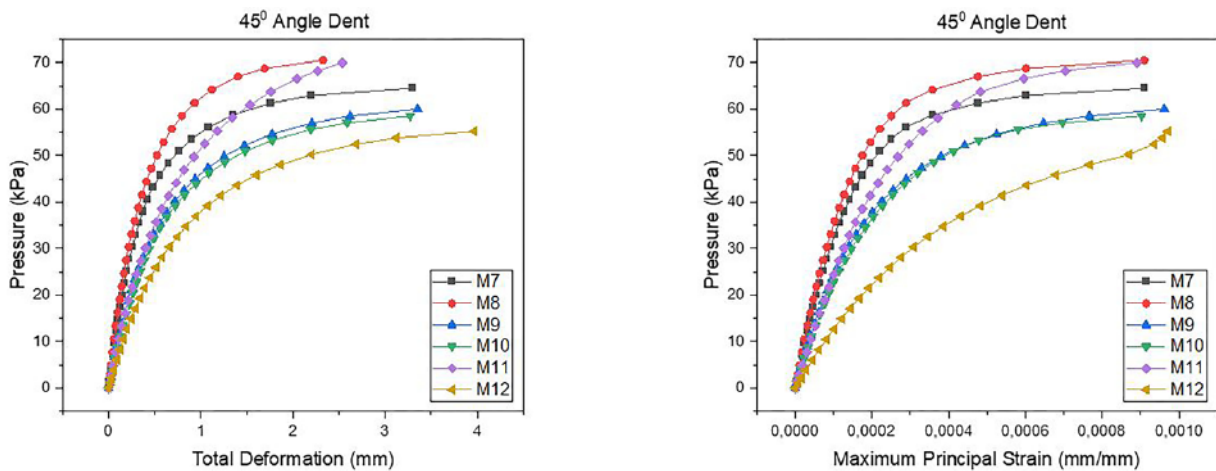


Figure 7.  
45°-angle dent group results

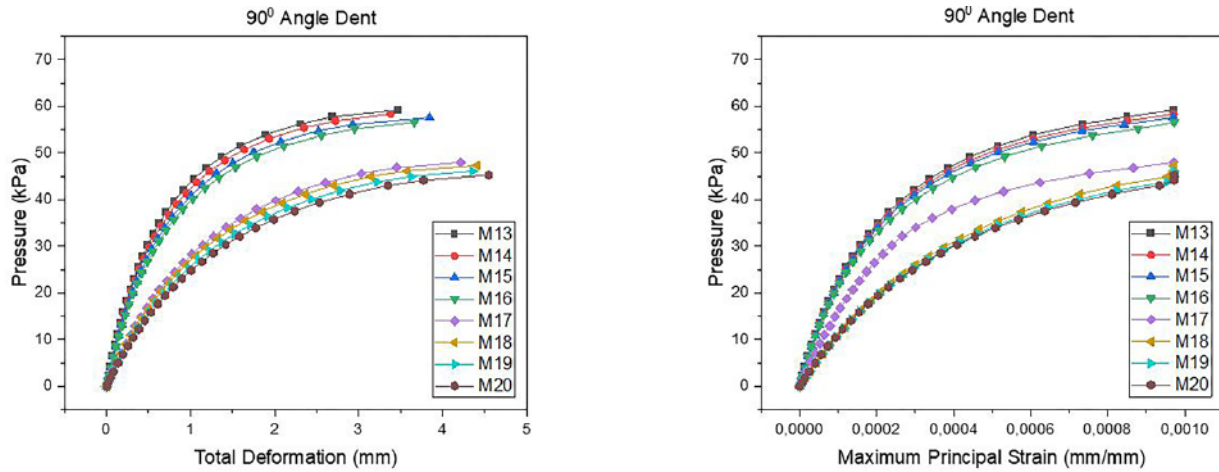


Figure 8.  
90°- angle dent group results

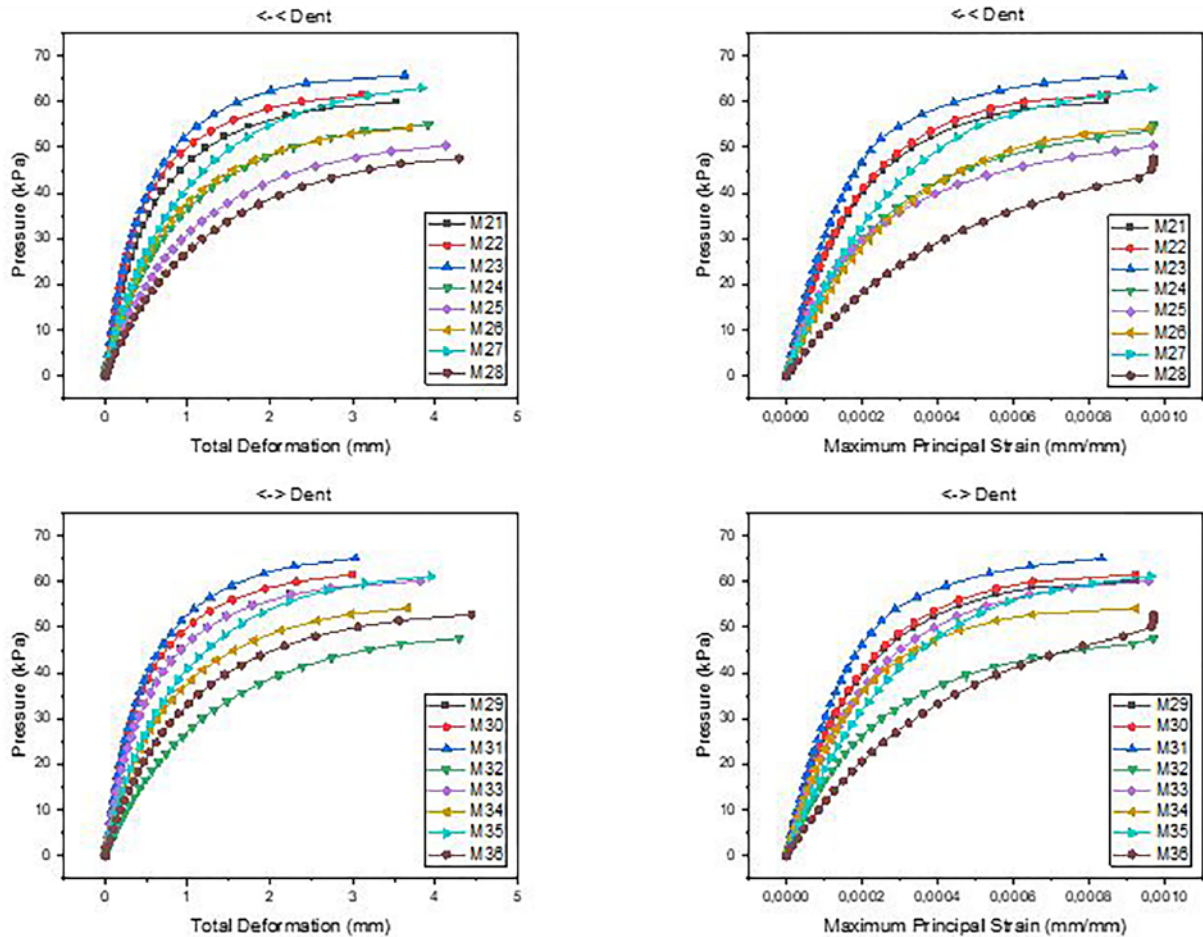


Figure 9.  
<-< and <-> dent shape group results

the critical buckling pressure in the models. But as it increased from  $h/3$  to  $h/2$  (from M2 to M3 and M5 to M6), the critical buckling pressure increased. The buckling wave numbers ranged from 6–7. Load-defor-

mation and load-strain graphs of the first group are given in Fig. 6. The M3 and M6 models are quite distinctive in the group. The FE results of this first group are shown in Table 4.

In the second group (45°-angle dent), only the critical buckling pressure of the M8 model is higher than the perfect model. Among the models with the same dent length and different dent widths, the dent width had a reducing effect on the critical buckling pressure. The dent length increased the critical buckling pressure from  $h/4$  to  $h/3$  and decreased it from  $h/3$  to  $h/2$ . The buckling wave numbers ranged from 6–8. Load-deformation and load-strain graphs of the second group are given in Fig. 7. The FE results of this second group are shown in Table 5.

The critical buckling pressure decreased from 0 to 90°-dent angles. In the third group (90°-angle dent), the critical buckling pressure decreased as the dent widths increased, similar to the other two groups. The dent length reduced the critical buckling pressure from  $h/4$  to  $3h/4$ . The buckling wave numbers were 6 and their shapes were nearly identical. Load-deformation and load-strain graphs of the third group are given in Fig. 8. The FE results of this third group are shown in Table 6.

In models with depth  $t$ , the angle increased from 0° to 90°, while the critical buckling pressures decreased at  $h/4$  and  $h/2$  dent lengths, while the critical buckling pressure increased from 0° to 45° in dents of length  $h/3$ , and the critical buckling pressure decreased from 45° to 90°. In models with  $2t$  depth, the critical buckling pressures decreased from 0° to 45°, whereas the critical buckling pressure increased from 45° to 90° for dent lengths  $h/4$ ,  $h/3$ , and  $h/2$ .

The last two groups had <-shaped dents. The dents belonging to the fourth group were both in the same

direction. In models with the same dent length, increasing the dent width in models with  $h/3$  (M21 and M25) and  $3h/4$  (M24 and M28) lengths decreased the critical buckling pressure. In other models (M22 and M26, M23 and M27), the dent width increased the critical buckling pressure. Increasing the dent length decreased the critical buckling pressure in  $h/4$ - $h/3$ - $3h/4$  lengths in  $t$ -width models, while it increased the critical buckling pressure in the  $h/2$  model. In models with a  $2t$  width, the critical buckling pressure increased from  $h/4$  to  $h/2$  and decreased again at  $3h/4$ . The buckling wave numbers ranged from 6–8. In the fifth group, the <-dents were designed in different directions. The critical buckling pressure of the  $H/4$  dent and  $t$ -width model was nearly identical to the critical buckling pressure of the  $2t$ -width model. In models with  $h/3$  and  $3h/4$  dent sizes, increasing dent width increased the critical buckling pressure. In models with  $h/2$  dent length, the critical buckling pressure decreased with increasing width. Increasing the dent length decreased the critical buckling pressure in  $h/4$ - $h/3$ - $3h/4$  models, while it increased the critical buckling pressure in  $h/2$  models. The buckling wave numbers were 6. Load-deformation and load-strain graphs of the fourth and fifth groups are given in Fig. 9. The FE results of both groups are shown in Table 7 and Table 8.

In general, dent geometries with the highest critical buckling pressure within each group were determined. These were the M6 (0°- $2t$ - $h/2$ ), M8 (45°- $t$ - $h/3$ ), M13 (90°- $t$ - $h/4$ ), M27 (<- $2t$ - $h/2$ ) and M31 (<- $t$ - $h/2$ ) models (<-< : symmetrical and concen-

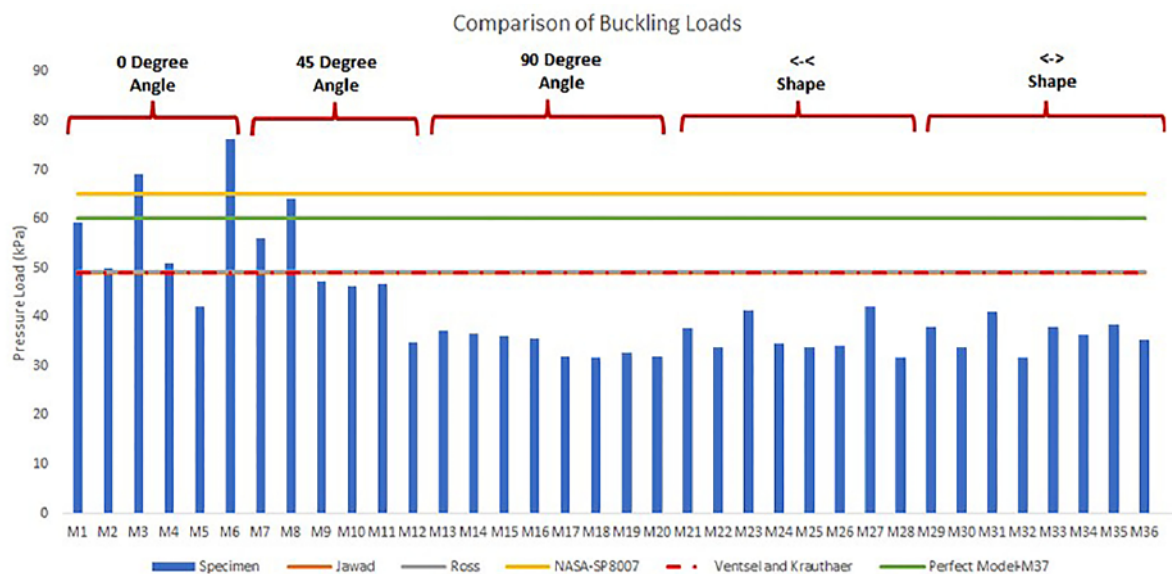


Figure 10. Comparison of critical buckling pressure values according to theory and codes

tric <-shaped dent, <-> : symmetrical and reverse <-shaped dent).

#### 4. COMPARISON

In this section, critical buckling pressure values in FE are compared with theoretical formulas and a perfect model. As can be seen in Fig. 10, the  $P_{cr}$  value of the perfect model in FE was among the  $P_{cr}$  values obtained from the formulas produced for perfect shells.

In Fig. 11, the variation in  $P_{cr}$  values of all models compared to the perfect model is shown. When the results obtained from the theoretical formulas given for the perfect models are examined, it is seen that the M37 (perfect model) model is the closest NASA-SP8007 formula to the critical buckling pressure value. The critical buckling pressure values of the M3 and M6 models were found to be higher than the values obtained from all the theoretical formulas given for the perfect models. Models with critical buckling pressure values exceeding the values obtained from Jawad, Ross, Ventsel and Krauthaer formulas are M1, M2, M3, M4, M6, M7 and M8. The critical buckling pressure values of all other models are lower than both M37 (perfect model) and theoretical pres-

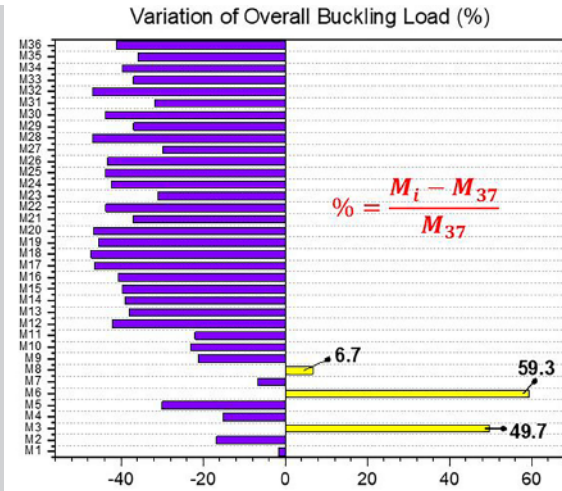


Figure 11. Effect of dent shape on buckling performance compared to the perfect model

sure values. While an increase was observed in the overall buckling pressures in the M3, M6, and M8 models, a decrease of 1.61–47.3% was detected in all other models compared to the overall buckling pressure of the perfect model.

Table 4.  
0°-angle dent shape results

	M1 (0°-t-h/4)	M2 (0°-t-h/3)	M3 (0°-t-h/2)	M4 (0°-2t-h/4)	M5 (0°-2t-h/3)	M6 (0°-2t-h/2)
Dent						
Total Deformation						
Max. Principal Strain						
Von Mises						
Waveforms						



**Table 5.**  
**45°-angle dent shape results**

	M7 (45°-t-h/4)	M8 (45°-t-h/3)	M9 (45°-t-h/2)	M10 (45°-2t-h/4)	M11 (45°-2t-h/3)	M12 (45°-2t-h/2)
Dent						
Total Deformation						
Max.Principal Strain						
Von Mises Stress						
Waveforms						

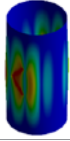
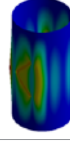
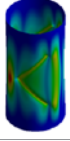
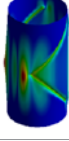
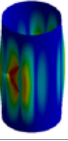
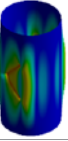
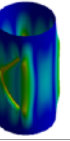
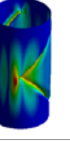
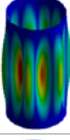
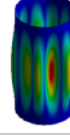
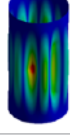
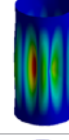
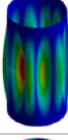
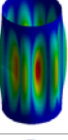
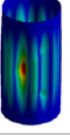
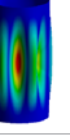
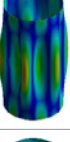
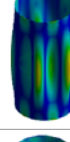
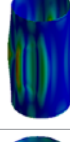
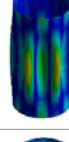
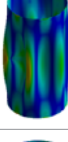
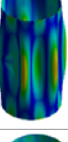
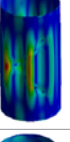
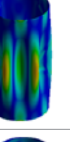
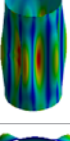
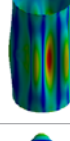
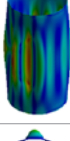
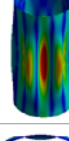
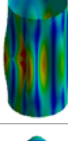
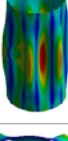
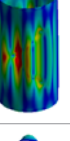
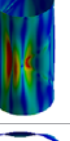
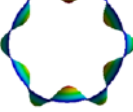
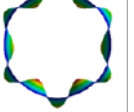
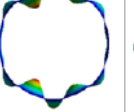
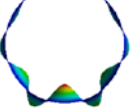

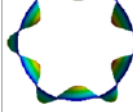
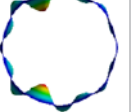
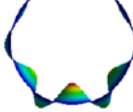
**Table 6.**  
**90°-angle dent shape results**

	M13 (90°-t-h/4)	M14 (90°-t-h/3)	M15 (90°-t-h/2)	M16 (90°-t-3h/4)	M17 (90°-2t-h/4)	M18 (90°-2t-h/3)	M19 (90°-2t-h/2)	M20 (90°-2t-3h/4)
Dent								
Total Deformation								
Max.Principal Strain								
Von Mises Stress								
Waveforms								



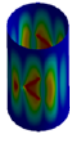
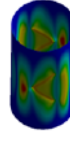
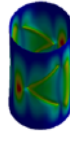
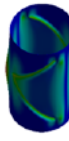
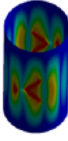
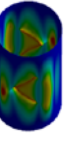
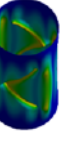
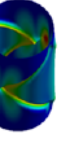
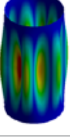
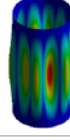
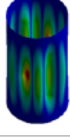
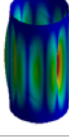
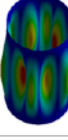
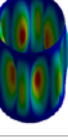
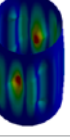
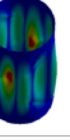
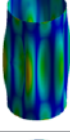
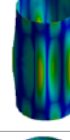
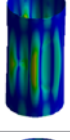
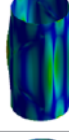
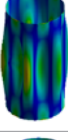
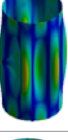
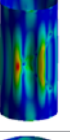
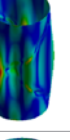
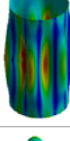
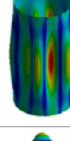
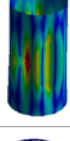
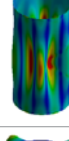
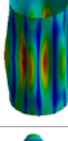
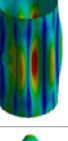
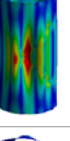
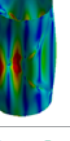

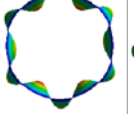
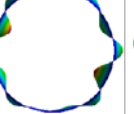
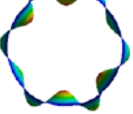
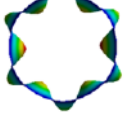
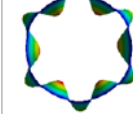
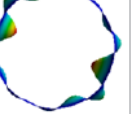
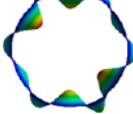
**Table 7.**

**<-< dent shape results**

	M21 (<<-t-h/4)	M22 (<<-t-h/3)	M23 (<<-t-h/2)	M24 (<<-t-3h/4)	M25 (<<-2t-h/4)	M6 (<<-2t-h/3)	M27 (<<-2t-h/2)	M28 (<<-2t-3h/4)
Dent								
Total Deformation								
Max.Principal Strain								
Von Mises Stress								
Waveforms								

**Table 8.**

**<-> dent shape results**

	M29 (<->-t-h/4)	M30 (<->-t-h/3)	M31 (<->-t-h/2)	M32 (<->-t-3h/4)	M33 (<->-2t-h/4)	M34 (<->-2t-h/3)	M35 (<->-2t-h/2)	M36 (<->-2t-3h/4)
Dent								
Total Deformation								
Max.Principal Strain								
Von Mises Stress								
Waveforms								

## 5. CONCLUSION

This present paper is a numerical study of the ultimate strength of dented cylindrical shells under external pressure of 37 thin-walled cylinders, 36 dented and a perfect model, with 5 different notch groups as reference. The conclusions are made based on FE analysis carried out on thin cylindrical shells with a dent of different shapes, sizes and angles of dent at 1/4-1/3/1/2-3/4 of the height of cylindrical shell taken for study.

- The NASA formula provided the closest value to the critical buckling load of the perfect model.
- Along the entire circumference dents increase critical buckling pressure.
- Thin cylindrical shells with circumferential dents have higher buckling strengths than cylindrical shells with longitudinal dents. As the dent angle increased towards 90-degrees, the critical buckling pressures decreased.
- Stresses are concentrated around the center of the dents. The strains were concentrated at the edges adjacent to the dents and less at the dent ends.
- All models were sensitive to parameters (width-depth-length-angle-shape).
- For models with dents, buckling was initiated from the dented area. A stiffener effect was observed in some dents. Both models with a dent along the entire circumference and a model with a 45-degree angle increased the critical buckling pressure.
- The buckling wave numbers were theoretically 6. In the FE results, the number of waves was between 6 and 8. The differences may be because buckling occurs in mode transitions in some models. But overall, the theory and simulation results were quite similar.

Overall, the study provides important insights into the behaviour of thin-walled steel cylinders with dents and offers a promising approach to enhancing the longevity and safety of structures through the transformation of dents into artificial stiffeners. The findings of this research can have significant implications for various industries, including aerospace, automotive, and construction.

## DECLARATION OF CONFLICT OF INTERESTS

The authors declare that there is no conflict of interest. They have no known competing financial interests or personal relationships that could have appeared to influence the work reported in this paper.

## NOMENCLATURE

- $\sigma$  – Tensile Strength
- $L_d$  – Dent length
- $b_d$  – Dent width
- $t$  – Thickness of cylinder
- $h_c$  – Height of cylinder
- $R$  – Radius
- $M_i$  – Model  $i$  ( $M_1, M_2, \dots, M_{37}$ )
- $P_J$  – Critical load of external pressure from Jawad theory
- $P_R$  – Critical load of external pressure from Ross theory
- $P_{VK}$  – Critical load of external pressure from Ventsel and Krauthaer
- $P_{SP-8007}$  – Critical load of external pressure from NASA SP-8007
- $P_{LBA}$  – Linear Bifurcation Analysis
- $r_m$  – Mean value of the radius
- $n$  – Number of circumferential buckling waves
- $E$  – Young's modulus
- $E_T$  – Tangent modulus

## REFERENCES

- [1] Zeybek, Ö. (2022). The stability of anchored cylindrical steel tanks with a secondary stiffening ring. *International Journal of Pressure Vessels and Piping*, 198, 104661.
- [2] Zeybek, Ö., & Özkılıç, Y. O. (2023). Effects of reinforcing steel tanks with intermediate ring stiffeners on wind buckling during construction. *Journal of Constructional Steel Research*, 203, 107832.
- [3] Chen, L., Rotter, J. M., & Doerich, C. (2011). Buckling of cylindrical shells with stepwise variable wall thickness under uniform external pressure. *Engineering structures*, 33(12), 3570–3578.
- [4] Broggi, M. S. G. I., & Schuëller, G. I. (2011). Efficient modeling of imperfections for buckling analysis of composite cylindrical shells. *Engineering Structures*, 33(5), 1796–1806.
- [5] Ghazijahani, T. G., Jiao, H., & Holloway, D. (2014). Experimental study on damaged cylindrical shells under compression. *Thin-Walled Structures*, 80, 13–21.
- [6] Ghazijahani, T. G., Jiao, H., & Holloway, D. (2014). Experiments on dented cylindrical shells under peripheral pressure. *Thin-Walled Structures*, 84, 50–58.

- [7] Gerasimidis, S., Viot, E., Hutchinson, J. W., & Rubinstein, S. M. (2018). On establishing buckling knockdowns for imperfection-sensitive shell structures. *Journal of Applied Mechanics*, 85(9).
- [8] Fatemi, S. M., Showkati, H., & Maali, M. (2013). Experiments on imperfect cylindrical shells under uniform external pressure. *Thin-Walled Structures*, 65, 14-25.
- [9] Aydin, A. C., Maali, M., Kiliç, M., Bayrak, B., & Akarsu, O. (2023). A numerical perspective for CFRP wrapped thin walled steel cylinders. *Steel Construction*. Article in Press.
- [10] Pan, J., & Liang, S. (2020). Buckling analysis of open-topped steel tanks under external pressure. *SN Applied Sciences*, 2(4), 535.
- [11] Chen, L., Rotter, J. M., & Doerich-Stavridis, C. (2012). Practical calculations for uniform external pressure buckling in cylindrical shells with stepped walls. *Thin-Walled Structures*, 61, 162-168.
- [12] Korucuk, F. M. A., Maali, M., Kiliç, M., & Aydin, A. C. (2019). Experimental analysis of the effect of dent variation on the buckling capacity of thin-walled cylindrical shells. *Thin-walled structures*, 143, 106259.
- [13] Rathinam, N., & Prabu, B. (2015). Numerical study on influence of dent parameters on critical buckling pressure of thin cylindrical shell subjected to uniform lateral pressure. *Thin-Walled Structures*, 88, 1-15.
- [14] Ghazijahani, T. G., Dizaji, H. S., Nozohor, J., & Zirakian, T. (2015). Experiments on corrugated thin cylindrical shells under uniform external pressure. *Ocean Engineering*, 106, 68-76.
- [15] Zeybek, Ö. (2022). The stability of anchored cylindrical steel tanks with a secondary stiffening ring. *International Journal of Pressure Vessels and Piping*, 198, 104661.
- [16] Jawad, M. (2012). *Theory and design of plate and shell structures*. Springer Science & Business Media.
- [17] Ross, C. T. (2011). *Pressure vessels: external pressure technology*. Elsevier.
- [18] Ventsel, E., Krauthammer, T., & Carrera, E. J. A. M. R. (2002). Thin plates and shells: theory, analysis, and applications. *Appl. Mech. Rev.*, 55(4), B72-B73.
- [19] Seide, P., Weingarten, V., & Petersen, J. (1965). NASA/SP-8007, Buckling of thinwalled circular cylinders. Nasa Space Vehicle Design Criteria (Structures).
- [20] Teng, J. G., Zhao, Y., & Lam, L. (2001). Techniques for buckling experiments on steel silo transition junctions. *Thin-Walled Structures*, 39(8), 685-707.
- [21] Aydin, A. C., Maali, M., Kiliç, M., Bayrak, B., & Akarsu, O. (2023). A numerical perspective for CFRP wrapped thin walled steel cylinders. *Steel Construction*.
- [22] ANSYS, I., *Workbench user's guide*. 2016, Release.
- [23] Song, C. Y., Teng, J. G., & Rotter, J. M. (2004). Imperfection sensitivity of thin elastic cylindrical shells subject to partial axial compression. *International Journal of Solids and Structures*, 41(24-25), 7155-7180.
- [24] Cai, M., Holst, J. M. F. G., & Rotter, J. M. (2002, June). Buckling strength of thin cylindrical shells under localized axial compression. In EM2002, 15<sup>th</sup> ASCE Engineering Mechanics Conference (pp. 2-5). New York: Columbia University.
- [25] Prabu, B., Raviprakash, A. V., & Venkatraman, A. (2010). Parametric study on buckling behaviour of dented short carbon steel cylindrical shell subjected to uniform axial compression. *Thin-Walled Structures*, 48(8), 639-649.
- [26] Gardner, L., & Ashraf, M. (2006). Structural design for non-linear metallic materials. *Engineering structures*, 28(6), 926-934.
- [27] Combescure, A., & Gusic, G. (2001). Nonlinear buckling of cylinders under external pressure with nonaxisymmetric thickness imperfections using the COMI axisymmetric shell element. *International Journal of Solids and Structures*, 38(34-35), 6207-6226.
- [28] Windenburg, D. F., & Trilling, C. (1934). Collapse by instability of thin cylindrical shells under external pressure. *Trans. Asme*, 11, 819-825.